Combined upsampling and denoising for diffusion MRI data

Samuel St-Jean, Max Viergever and Alexander Leemans
Image Sciences Institute, University Medical Center Urecht, Utrecht, The Netherlands

Introduction

Diffusion MRI (dMRI) suffers from relatively long scan times and low signal to noise ratio (SNR), which limits the acquired spatial resolution. Many techniques have emerged to increase image quality and achieve higher spatial resolutions such as specialized acquisition schemes [1, 2, 3], image processing techniques to increase spatial resolution [4, 5, 6] and denoising techniques to increase the SNR [7, 8, 9].While these methods typically aim to either increase the spatial resolution *or* improve the SNR, it would be beneficial to combine both, enhancing their effectiveness. In this work, we propose such a unified framework for denoising and upsampling dMRI data based on a sparse representation of the diffusion signal.

Theory

Sparse linear models have been used as a powerful method to represent the MRI signal by only using a few elements. Such a representation has been used for structural MRI upsampling [10] or dMRI denoising [8]. The key idea is to decompose locally n dMRI signals X_i as a linear combination of a few basis elements [11] through **equation 1**. By exploiting the redundancy of the signal, a sparse representation $X_i=\mathbf{D}\alpha_i$ can be found, with X_i the MRI signal in a neighborhood i, **D** the dictionary, α_i the sparse coefficients, a tradeoff parameter between data fitting and sparsity and X_i the reconstructed signal. In our unified framework, we propose to extract a lower resolution representation **d** by averaging the columns of **D** to form smaller patches, thus giving a one-to-one mapping between low and high resolutions patches within a multiscale approach [12]. We then solve **equation 2** using **d** with $\lambda_i=\sigma^2_i$ (m + 3√2), and m the number of elements in a patch. This would give a denoised representation [8] for $X_i=\mathbf{d}\alpha_i$, but by instead using the direct relationship between **d** and **D**, we reconstruct a high resolution, denoised representation $\hat{X} = D\alpha_i$ as shown schematically in **figure 1.**

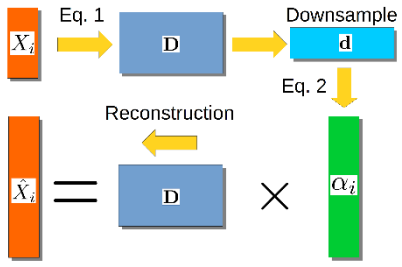

Figure 1: Schematic representation of the proposed framework. The dictionary D is computed with equation 1 and downsampled into d, creating an exact mapping between the low and high resolution elements. αi is then computed with equation 2 and d, which gives the final denoised and upsampled reconstruction using $\hat{X} = D\alpha_i$.

Methods

Two datasets of the same subject were obtained on the same 3T Philips scanner; a 1.8 mm dataset with 64 b = 1000 s/mm^2 volumes, TR/TE = 18.9 s / 104 ms and a 1.2 mm dataset with 40 b = 1000 s/mm^2 volumes, TR/TE = 11.1 s / 63 ms, both with one b = 0 s/mm^2. The 1.2 mm dataset serves as a gold standard for spatial resolution attainable with enough signal within a reasonable timeframe on a standard scanner. Using the 1.8 mm dataset, we first estimated the variance of the Rician noise with PIESNO [13] and corrected for Rician noise bias [14]. We extracted spatial patches of size (6, 6, 6) with 5 angular q-space neighbors to construct **D** using **equation 1** and then downsampled it by a factor of 2 in each dimension, thus creating d of size (3, 3, 3). The coefficients i were computed with **equation 2** and **d**, thus obtaining an upsampled $\hat{X} = D\alpha_i$ at 0.9 mm. To show the improvements of the proposed method, we denoised separately the 1.8 mm and 1.2 mm datasets. The original 1.8 mm and denoised datasets were then upsampled by a factor 2 using both linear spline and cubic spline interpolation as described previously [5]. We also computed colored fractional anisotropy (FA) maps with a robust tensor estimation [15] as implemented in ExploreDTI [16].

Results

Figure 2 compares the raw data on the 1.8 mm dataset and the various upsampling on the original and denoised dataset on a coronal slice. The 1.2 mm dataset is also shown with its denoised version for anatomical comparison. **Figure 3** shows two zoomed regions; the corpus callosum, the cingulum and the corticospinal tract and the pons region with the cerebellum. **Figure 4** and **5** show the colored FA maps of the previous figures. Interpolation on the raw data leads to residual artefacts in the interpolated dataset. Applying denoising separately from interpolation introduces line artefacts or blurring, while our proposed combined approach preserves more details, but with the tradeoff of some blocking artefacts. Interpolation results are in agreement with the 1.2 mm raw and denoised dataset, even though they are produced from a 1.8 mm dataset.

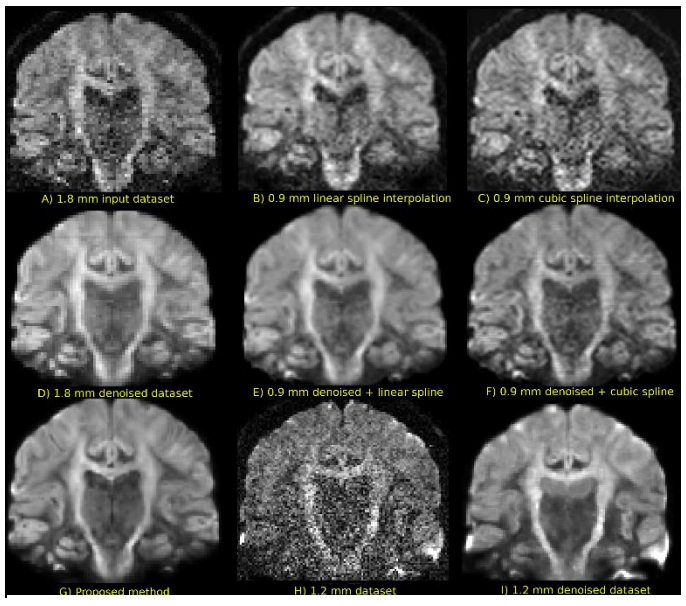

Figure 2: **Top row**: interpolation only. **Middle row**: denoising and interpolation. **Bottom row**: proposed method and comparative denoised 1.2 mm dataset. Interpolating the noisy data picks up most of the noise, while interpolating the denoised data is more blurry than our proposed framework.

Discussion and conclusion

We presented a new framework which combines two usually separate processing steps, namely denoising and upsampling, in a single unified framework. The proposed method links a set of lower and higher resolution patches, which permits reconstruction of dMRI data at a higher resolution than initially acquired without using specialized acquisition schemes. This category of approaches is particularly attractive since they can be applied on any already acquired datasets. As noted previously [5], upsampling can reveal finer anatomical details which might help tractography, but care should be taken about possible biases or introduced artefacts in computed metrics such as FA. Moreover, our proposed method could be combined with acquisition techniques [1, 2, 3] to potentially improve the provided anatomical information.

References

1. Ning, L. et al., 2016 *NeuroImage* 2. Scherrer, B. et al., 2015. *Information Processing in Medical Imaging* 3. Van Steenkiste, G. et al., 2016. *Magnetic Resonance in Medicine* 4. Coupé, P. et al., 2013. *NeuroImage* 5. Dyrby, T.B. et al., 2014. *NeuroImage* 6. Yap, P.T. et al., 2014. *NeuroImage* 7. Manjón, J. V. et al., 2010. *J. Magn. Reson. Imaging* 8. St-Jean, S. et al., 2016. *Medical Image Analysis* 9. Veraart, J. et al., 2016. *NeuroImage* 10. Rueda, A., et al., 2013. *Medical image analysis* 11. Mairal, J. et al., 2009. *The Journal of Machine Learning* 12. Glasner, D., et al. 2009. *International Conference on Computer Vision (ICCV)* 13. Koay, C.G., et al, 2009. *Journal of Magnetic Resonance* 14. Koay, C.G., et al., 2009. 15. Tax, C. M.W., et al., 2015. *Magn. Reson. Med.* 16. Leemans A. et al., 2009. 17th Annual Meeting of *Intl. Soc. Mag. Reson. Med.*

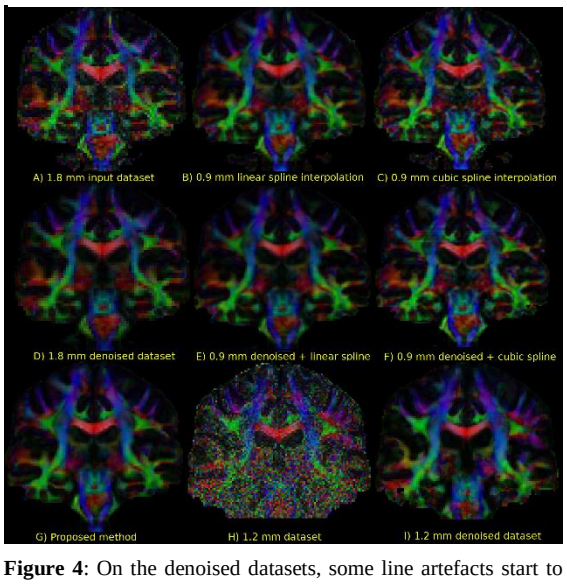

Figure 4: On the denoised datasets, some line artefacts start to appear and are more common in the cubic spline interpolated version. In contrast, our proposed method does not seem to exhibit such issues and is in agreement with the denoised 1.2 mm dataset, notably in the pons region.

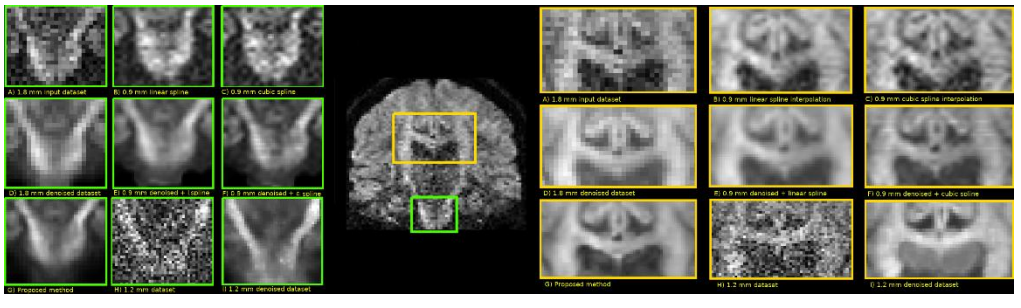

Figure 3: In the pons, interpolation with or without denoising shows more blurring than the 1.2 mm denoised acquisition than our proposed method. The contrast between the corpus callosum, the ventricles and the corticospinal tract is preserved with our proposed method, but lost with the linear and cubic spline interpolation.

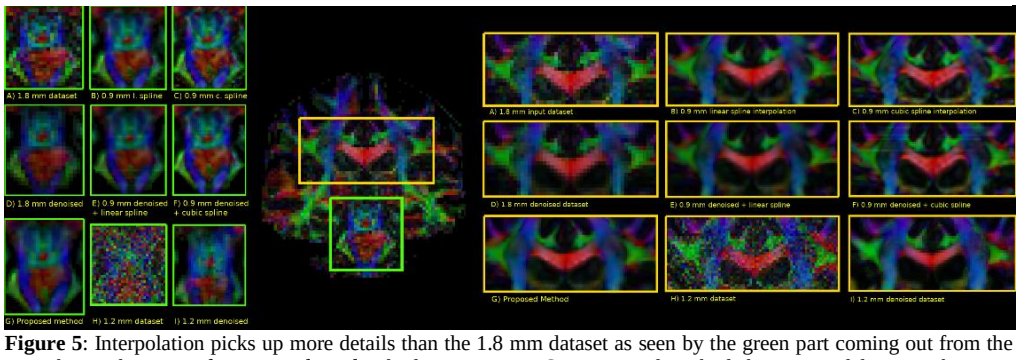

Figure 5: Interpolation picks up more details than the 1.8 mm dataset as seen by the green part coming out from the pons, but at the price of some artefacts for the linear version. Our proposed method shows nice delineation between the different structures, similar to the 1.2 mm dataset.